

Original Research

Study of CO₂ Emissions from Traffic and CO₂ Sequestration by Vegetation Based on Eddy Covariance Flux Measurements in Suburb of Beijing, China

Yu Li¹, Jing Gao^{1*}, Suocheng Dong^{1,2}, Ji Zheng^{1,2}, Xin Jia³

¹Institute of Geographic Sciences and Natural Resources Research, Chinese Academy of Sciences, Beijing 100101, China

²College of Resources and Environment, University of the Chinese Academy of Sciences, Beijing 100190, China

³School of Soil and Water Conservation, Beijing Forestry University, Beijing 100083, China

Received: 18 November 2018

Accepted: 19 January 2019

Abstract

Many studies have shown that urban forests function as important carbon (C) sinks by sequestering carbon dioxide (CO₂), and there are a great deal of scientific data on their potential to fix CO₂ through photosynthesis, including variations among vegetation types and temporal dynamics. However, although vehicle traffic is one of the main anthropogenic sources of CO₂, the relationship between these emissions and sequestration by vegetation is unclear. Here, we use the eddy covariance technique to directly measure the net CO₂ flux to: (1) quantitatively validate C emissions from transportation and C sequestration by vegetation at the spatio-temporal resolution of 1 km and 30 min and (2) select tree species that best sequester C by photosynthesis and identify the major controlling factors. During the daytime monitoring period (7:00-17:00) of the plant-growing season (May-October), the net photosynthetic C sequestration per tree was used to measure the C fixation capacity of different tree species, and the order was Mono maple > Amur cork tree > Goldenrain > Chinese ash > Chinese pine > Ginkgo. In the study, C sequestration by trees was primarily controlled by photosynthetically active radiation, traffic volume and relative humidity, which together explained 92.3% of the total C sequestration by trees during the monitoring period in the growing season, and C sequestration was positively correlated with photosynthetically active radiation and traffic flow, but negatively correlated with relative humidity. Furthermore, vehicle CO₂ emissions significantly increased the amount of photosynthetic C sequestration due to a fertilization effect. Therefore, it is necessary to improve the accuracy of micro-scale regional C flux measurements in order to more accurately determine CO₂ sources and sinks and inform the selection of vegetation that can maximize the sequestration of traffic CO₂ emissions.

Keywords: CO₂ emissions from transportation, CO₂ fluxes, CO₂ sequestration by vegetation, fertilization effect

Introduction

Urban areas and the rapid progress of industrialization and technology are leading to serious air pollution in urban areas. In particular, human beings trying to maintain an urban life style harm health [1-5]. In Europe, more than two-thirds of the total population lives in cities. Population growth and industrialization have led to air pollution in some cities that reaches levels that threaten human health. This has become one of the most important topics of our day. Human health is affected by all air pollution, but some emissions have more severe atmospheric conditions. In particular, carbon dioxide (CO₂) and other pollutants, which fuel global warming, have recently attracted attention because CO₂ is one of the most researched gases [6-10].

Many studies have shown that carbon dioxide (CO₂) is one of the most important greenhouse gases, which are the primary cause of global warming and climate change [11-15]. While urban areas – the main sources of CO₂ emissions – occupy less than 2.4% of the total surface area of the earth, they contribute 80% of anthropogenic CO₂ emissions [16]. In addition, according to estimates from the International Energy Agency, CO₂ emissions from the transportation sector account for 23% of global CO₂ emissions [17], ranking behind emissions from the electricity sector and heating systems, and this proportion will rise to 50% by 2030 and to 80% by 2050 [18]. In particular, by the end of 2016, the number of motor vehicles in Beijing was 5.72 million with a growth rate of 1.7% [19] (Beijing Municipal Bureau of Statistics), causing CO₂ emissions from traffic to continue to rise rapidly, which will lead to extreme weather events, drought and rainstorm due to climate warming that will affect food security and human health as well as social security and stability [20].

Currently, global warming and climate change caused by increasing CO₂ emissions are major issues of concern for the international community. In 1997, the Kyoto Protocol was drafted during the Third Conference of the Parties (COP-3) of the United Nations Framework Convention on Climate Change (UNFCCC), and it was the first international provision with legally binding force to quantify carbon (C) reduction targets for developed and developing countries. More importantly, the Kyoto Protocol proposed that C reduction could be achieved by decreasing the use of fossil fuels or by the sequestration of C in the vegetation and soils of terrestrial ecosystems. As an important part of urban ecosystems, city forests have been recognized by the international community as playing a critical role in CO₂ sequestration and the mitigation of climate warming [21, 22]. Therefore, city greening measures are a widespread response to climate change, and many local governments have adopted practices such as afforestation, the expansion of city green space policies, and the continuous improvement of urban forest C-compensation standards and terms to quantify CO₂ sequestration by vegetation [23-26].

However, due to the limited availability of data related to the spatial and temporal dynamics of C at local scales, the relationship between C sequestration and C source assessments tend to be on the large scale. Specifically, allometric equations incorporating vegetation volume (tree height and diameter at breast height (DBH)) and vegetation inventory data are used to predict vegetation C sequestration based on the growth-model method [27-30], and traffic emissions are estimated by the CO₂ emission inventory method (reference documents or transportation industry reports). The spatial scale is typically a city, and the time scale is a year [29-32]. In the city of Bolzano, Italy, Russo et al. (2015) used plant allometric equations and vegetation inventory data at the city-block scale and found that C sequestration by vegetation offsets 0.08% of the CO₂ emissions from traffic [29]. Gratani and Varone (2014) found that the atmospheric CO₂ concentration was positively correlated with the volume of traffic and negatively correlated with the scale of a city park [31]. These results indicate that urban vegetation plays an important role in the sequestration of traffic CO₂ emissions. However, the present studies about CO₂ emissions from traffic and CO₂ sequestration by vegetation lack the dynamic characteristics of vegetation photosynthesis and traffic flow, and the comparison of carbon sequestration capacity between tree species, which would be explored in this study.

Obviously, various empirical models based on longer time scales and static biomass C sequestration have simple and nondestructive characteristics, but the ideal model cannot reflect spatio-temporal differences in vegetation C-sequestration efficiency and are thus limited in their ability to reveal the mechanism underlying the sequestration of anthropogenic CO₂ emissions by vegetation [30, 33-35]. Moreover, because models usually do not directly use site or species-specific tree growth or mortality rates, most urban forest functional models will have sources of error [36]. Therefore, the spatial and temporal micro-scales of the photosynthetic C-sequestration efficiency of the vegetation and its influencing factors should be considered in predictive meteorological, satellite remote sensing and ecosystem C-sequestration models [37]. In addition, as a mobile pollution source, vehicle CO₂ emissions also exhibit significant spatial and temporal variations [38-40]. More importantly, many studies have shown that a short-term increase in the concentration of CO₂ can significantly increase vegetation sequestration of C during the day [41]. Therefore, the temporal and spatial variations in the efficiency at which traffic CO₂ emissions are sequestered by vegetation have become a hot research topic.

Eddy covariance flux measurement methods use meteorological data to directly monitor CO₂ flux, thus informing the screening and verification of CO₂ sources and sinks at a spatio-temporal scale of 10²–10⁴ m and 30 min [32, 42-46]. Using the eddy covariance technique and the allometric equation model, Velasco et al. (2013)

directly evaluated the potential sequestration of C by vegetation by simulating traffic CO₂ emissions with the MOVES2010 model, simulating the release of CO₂ by soil respiration with the Q10 model, and estimating the release of CO₂ from human respiration and buildings using a questionnaire survey and analyzing data from the literature; the difference between CO₂ emissions and the net C fluxes was the C sequestered by the vegetation [46]. Therefore, the study of Velasco et al. demonstrates that a combination of methods by using eddy covariance flux measurements to determine the spatial boundary of the contributing emissions, monitoring each part of the emission inventory at the micro scale, and simulating each component of the rate of carbon flux with a model that combines both emission inventory (inventory statistics) and direct monitoring (direct measurement) can be used to gain new insights into processes involved and to quantify their respective contributions.

This study used the eddy covariance flux technique and modeling to determine the boundary of the area contributing to C flux and to monitor vegetation photosynthesis, traffic flow in the study area at every half hour scale. Then the simulation model was used to determine the dynamic change in each component of the C flux in 30-min intervals, and correlation and regression analysis were used to identify the vegetation types that best sequester traffic CO₂ emissions and to verify the “fertilization effect” of vehicular CO₂ on the vegetation, which is of great significance for reducing urban CO₂ emissions.

Materials and Methods

Study Area

The study area is in Badaling Forest in Yanqing County, Beijing, China (40°22.38'N, 115°56.65'E) at an elevation of 535 m. The area is semi-arid with a semi-humid continental monsoon climate, and the mean annual temperature is 10.8°C with monthly average temperatures ranging from -7.2°C (January) to 26.9°C (July). The mean annual evaporation is 1586 mm, and the long-term mean annual precipitation is 450 mm, which is concentrated in July-August and accounts for approximately 59% of the total annual precipitation. The average annual relative humidity is 56.2%, and the average wind speed is 3.1 m·s⁻¹.

The forest density was 975 stems/ha, and the trees averaged 7 years in age with an average height of 6.0 m and an average DBH of 29.0 cm. The broad leaved trees in the forest are goldenrain (*Koelreuteria paniculata*), Chinese ash (*Fraxinus chinensis Roxb.*), amur cork tree (*Phellodendron amurense*), mono maple (*Acer truncatum Bunge*) and ginkgo (*Ginkgo biloba Linn.*), which account for 82.5% of the forest; the main coniferous species is Chinese pine (*Pinus tabulaeformis*), which accounts for 17.5% of the forest. The shrub layer is mainly composed of begonia flower (*Malus spectabilis*) and torch tree

(*Rhus typhina*). The herbs are mainly green bristlegrass (*Setaria viridis*), deyeuxia sylvatica (*Deyeuxia arundinacea*), lard mans (*Spodiopogon sibiricus*), and catchweed (*Galium aparine*); the total summer herb coverage varies from 20 to 30%.

Estimating CO₂ Emissions Using Bottom-up Approaches

The equation expressing the CO₂ flux between the underlying surface and the atmosphere is as follows:

$$FC = ET + EB + RH + (RS + RV - PV)$$

...where *FC* represents the net CO₂ flux; *ET* represents the CO₂ emissions from vehicle traffic; *EB* represents the CO₂ emissions from buildings; *RH* represents human respiration; *RS* represents the CO₂ emissions from soil respiration; *RV* represents the CO₂ released by ground vegetation at night; and *PV* represents the photosynthesis by ground vegetation during the day minus the CO₂ from respiration. Conventionally, a positive flux indicates the release of CO₂, and a negative flux indicates that the amount of CO₂ is fixed. The study area was located in a forest and included two forest management sites, a small airport and a small part of a residential area. Because the residents of the study area work during the day, the workers mostly use electrical equipment in the forest management sites, and the frequency of take-offs and landings at the airport is less than 5 times from 7:00 to 17:00, there are almost no direct CO₂ emissions except from traffic and the soil during daytime. In addition, the area contributing to the C flux contains a highway; therefore, we assume that the observed flux is the combination of *ET*, *RS*, *RV* and *PV* [46].

Eddy Covariance Flux Measurements and Footprint Analysis

A three-dimensional ultrasound instrument (CSAT3, Campbell Scientific Ltd., USA) was installed on a flux observation tower at 11.7 m above the ground and used to measure wind speed and the virtual fluctuation in temperature, and a closed-type infrared gas analyzer (EC155 Campbell Scientific Ltd., USA) was used to measure the fluctuations in the concentrations of CO₂ and water (H₂O). The turbulent fluctuation signal was recorded by a data acquisition unit (CR3000, Campbell Scientific, USA) at a 10-Hz sampling frequency.

A micro-meteorological observation system was installed on the tower, and it included 3 air temperature, humidity sensors (HMP45C, Campbell Scientific Ltd., USA) and sonic anemometer (CSAT-3, Campbell Scientific Ltd., USA), photosynthetically active radiation sensors (PAR-LITE, Kipp & Zonen, Netherlands) and a tipping-bucket rain barrel (TE525, Campbell Scientific Ltd., USA). Four soil temperature sensors (109, Campbell Scientific Ltd., USA) and 4 soil moisture sensors (CS616, Campbell Scientific Ltd.,

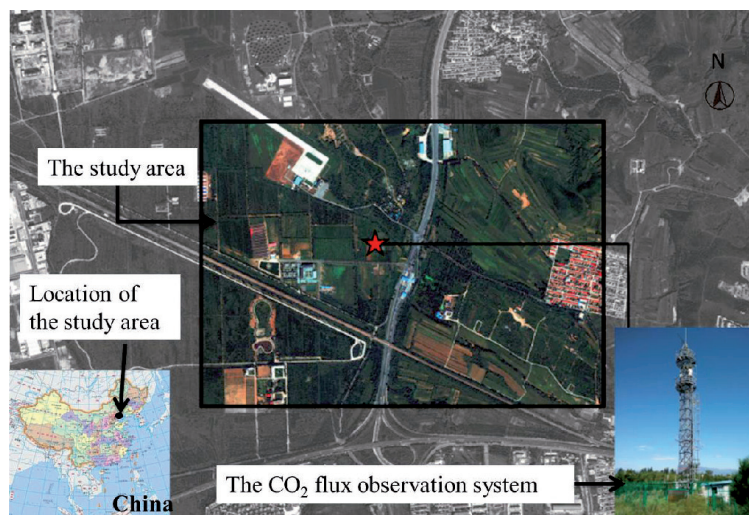


Fig. 1. Study area.

USA) were installed at a depth of 10 cm approximately 10 m away from the observation tower. Measurements were recorded at a 0.1-Hz sampling frequency by a data collector (CR1000, Campbell Scientific Ltd., USA), which provided a cumulative value for 30 min for the rain gauge or an average value for the other sensors. The zero values for CO_2 and H_2O were determined using a vortex system with highly pure nitrogen (N), and the CO_2 and the H_2O calibration was performed using a standard gas of $496 \mu\text{mol CO}_2 \cdot \text{mol}^{-1}$ dry air with 220 V of alternating current as the main power supply and a battery as the backup power supply [47].

The source area (Fig. 1) represents the portion of the flux tower that can be monitored to determine the CO_2 source/sink area using an analytical model of the flux data, which are measured every 30 min [48]. This analytical solution for the footprint model relies on the sophisticated formulation by van Ulden (1978) [49] using the parameterization methods in Gryning et al. (1987) [50], Finn et al. (1996) [51], and Kormann and Meixner (2001) [52], while accounting for atmospheric stability, which is related to the wind velocity above the canopy by a power law. This law applies to all conditions of atmospheric stability, and the inputs include the measurement height (z_m), displacement height (z_d), wind speed (u), wind direction, the standard deviation of the lateral wind speed (σ_v), the wind friction velocity (u^*) and the Monin-Obukhov stability (z/L , where L is the Obukhov length, and z is the effective measurement height: $z = z_m - z_d$). Based on the flux-tower data, which was monitored every 30 min for three days, and the above flux contribution model, the distances from the center of the flux tower to the four corners of the contributing area were obtained: north (625 m), south (975 m), east (1000 m) and west (775 m) (Fig. 1). The study area was the maximum footprint monitored by EC, which was 2.84 km^2 . Forest covered 71%, building covered 17%, bare land covered 9% and roads covered 3%.

CO₂ Emissions from Traffic

A camera (SONY, HDR-CX510E) with a high pan-tilt-zoom (PTZ) field was used to monitor traffic flow within the scope of the largest C-flux contribution area. To ensure that no vehicle was missed or that no vehicle blocked the line of sight, the camera instrument frame was placed 7 m from the ground overlooking the main road and side roads. The field-monitoring video that was taken between 7:00 and 17:00 on three random sunny days of every month from May to October, 2017 was used for visual interpretation; the number of vehicles (small, medium and large passenger cars; light, medium and heavy trucks; and buses) in the flux contribution area per 30 min was counted. Using a questionnaire survey, vehicle fuel consumption per 100 km (L/100 km) was obtained and multiplied by the IPCC (2007) emission factors to determine the CO_2 in the gasoline and the amount of CO_2 emissions per 100 km ($\text{g CO}_2 / 100 \text{ km}$), as well as the overall international $\text{g CO}_2 / \text{km}$ of the vehicles [53]. Finally, by multiplying the vehicle CO_2 emission factor by the number of vehicles in the contribution area per 30 min, the total CO_2 emissions per 30 min of traffic for the flux contribution region was obtained [53].

CO₂ Sequestration by Vegetation

A LI-6400/LI-6400 portable photosynthesis measurement system (LICOR Inc., USA) was used to measure the net photosynthetic rate (A , $\mu\text{mol} \cdot \text{m}^{-2} \cdot \text{s}^{-1}$) as well as other physiological indicators and environmental parameters, including atmospheric CO_2 concentration (C_{ref} , $\mu\text{mol} / \text{mol}$), air temperature (T_{ch} , $^{\circ}\text{C}$), photosynthetically active radiation (Q_{leaf} , $\mu\text{mol} \cdot \text{m}^{-2} \cdot \text{s}^{-1}$), leaf temperature (T_{l} , $^{\circ}\text{C}$), and humidity (e_{ref} , %) between 7:00 and 17:00 on three random sunny

days of every month from May to October, 2017 of six tree species with 3 replicates. The measurement interval was 30 min using the method of Biswas et al. [33].

Leaf Area Index

The leaf area index and the diurnal changes in photosynthesis were determined simultaneously using an LAI-2200 (LICOR Inc., USA) / Wins Canopy 2009a canopy analyzer assembly equipped with a digital camera with a fisheye lens. The specific measurement and calculation methods followed Biswas, and Wins Canopy 2009a canopy analyzer software was used to analyze the image, with the LAI equal to LAI (2000G)-Log CI [33].

Data Processing

According to the measured net photosynthetic rate values, the net assimilation rate of each tree species was calculated by simple integration:

$$p = \sum_{i=1}^j [(P_{i+1} + P_i) \div 2 \times (t_{i+1} - t_i) \times 3600 \div 1000]$$

...where P represents the total leaf area determined by the assimilation unit, $\text{mmol}\cdot\text{m}^{-2}\cdot\text{d}^{-1}$; P_i represents the initial measuring point of the instantaneous photosynthetic rate; and P_{i+1} is the next measuring point of the instantaneous photosynthetic rate in $\mu\text{mol}\cdot\text{m}^{-2}\cdot\text{s}^{-1}$ with the instantaneous time point, T_i , measured as early as t_{i+1} and the next time point as H .

The formula for calculating the daily C fixation of single tree is as follows:

$$W_{co_2} = w_{co_2} \times S_l = P \times 44 \div 1000 \times LAI \times S_l$$

... where w_{co_2} is the daily C sequestration ($\mu\text{mol}\cdot\text{m}^{-2}\cdot\text{s}^{-1}$) by the tree; S_l is the total leaf area per plant (m^2); W_{co_2} is the mass per unit area of leaf-fixed CO₂ ($\text{g}\cdot\text{m}^{-2}\cdot\text{d}^{-1}$); and 44 is the molar mass of CO₂ ($\text{g}\cdot\text{mol}^{-1}$). [54]

Statistical Analysis

The differences among the means were tested by one-way analysis of variance (ANOVA) and Tukey's test for multiple comparisons. Simple regression analysis was used to analyze the correlation between traffic and the anthropogenic CO₂ emissions after being checked for normality and transformed data, and a stepwise linear model with backward selection was applied to discriminate between the contributions of each variable to the C sequestered by the vegetation. In each case, the best model was chosen based on the R^2 values. All statistical tests were performed using SPSS 19.0.

Diurnal Variation in Environmental Factors

Plant photosynthesis is affected by environmental factors, including light, air temperature, atmospheric CO₂ concentration and relative humidity.

As shown in Fig. 2a), the trend of the change in photosynthetically active radiation was a curve with a single peak at 12:00 in every month from May to October, 2017. The maximum solar elevation angle and the strongest radiation occur at noon, when the plant receives the maximum amount of solar radiation energy. Therefore, the photosynthetically active radiation from 10:00-14:00 was maintained at a relatively high level while the sunlight intensity after 17:00 was insufficient to meet the needs for leaf photosynthetic activity. The results showed that the order of photosynthetic radiation in plant-growing season was July > August > June > May > September > October.

Changes in temperature are caused by changes in light intensity, which means that temperature increases with increasing light intensity, but there is a lag. As seen from Fig. 2b), the temperature reached its maximum value between 14:00 to 15:00 after the peak light intensity value was reached at 12:00. The temperature rose rapidly from 7:00-13:00 and then decreased very slowly between 15:00-17:00. The results showed that the order of temperature in plant-growing season was July > August > June > May > September > October.

As seen from Fig. 2c), the trend of the change in humidity was a curve with a single lowest point in the afternoon in every month from May to October, 2017. On the whole, the humidity in the morning was the maximum and then decreased sharply until afternoon, with a slight rise thereafter every month. Specifically, the humidity of July and August were higher than other months due to being in rainy season, as well as large amount of evaporation. By comparison, the humidity of May was the lowest throughout the daytime in plant-growing season.

The trend in the diurnal variation in the atmospheric CO₂ concentration was generally an inverted arc (Fig. 2d). The atmospheric CO₂ concentrations were similar with maximums at 7:00 and then decreased with time, reaching minimum values around 14:00 and rising slightly until 17:00. Obviously, the atmospheric CO₂ concentrations of October were always higher than any other months, which were between 445.48 ppm to 458.98 ppm. By comparison, the atmospheric CO₂ concentrations of June were the lowest among all months in plant-growing season, which were between 374.51 ppm to 395.99 ppm.

Carbon Sequestration Ability of the Tree Species

The daily C stored by the plants was calculated from the diurnal variation in the net photosynthetic rate of each tree species combined with the total leaf area per plant (Table 1). During the daytime monitoring period

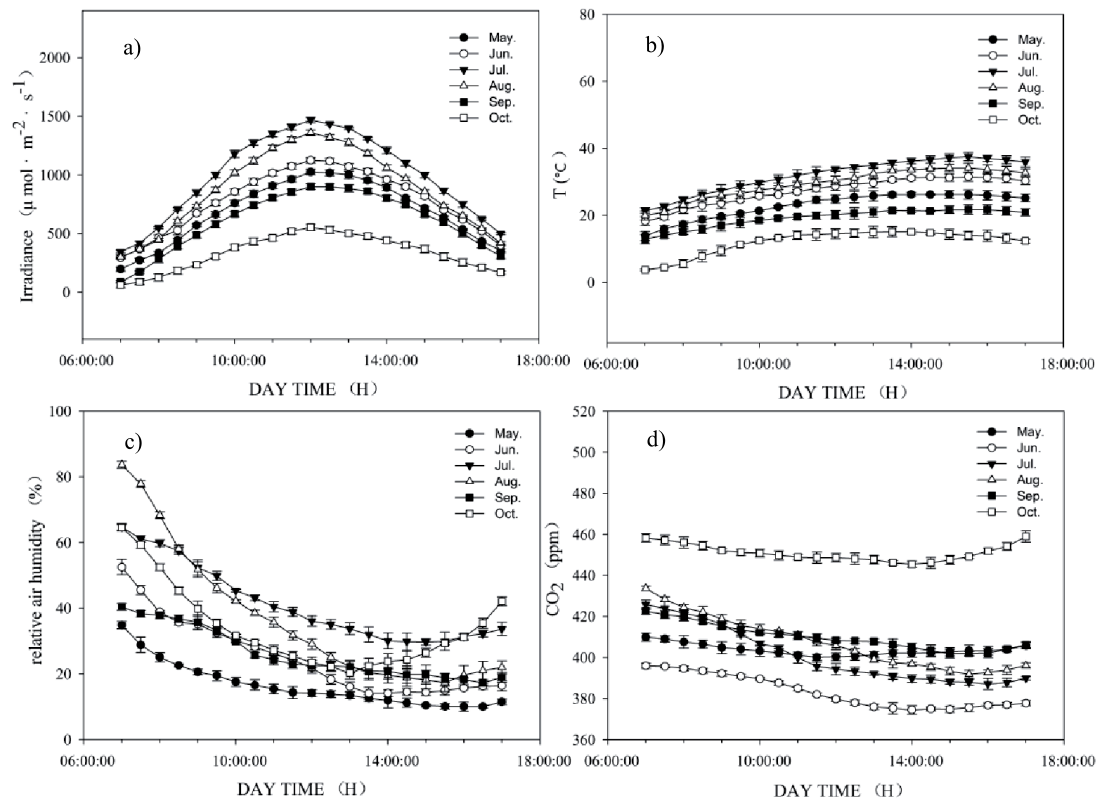


Fig. 2. Characteristics of the daily variation in photosynthetically active radiation a), temperature b), atmospheric relative humidity c) and atmospheric CO_2 concentration d) in plant-growing season (May-October).

(7:00-17:00) of plant-growing season (May-October), the order of net photosynthetic C sequestration per tree was Mono maple > Amur cork tree > Goldenrain > Chinese ash > Chinese pine > Ginkgo (Fig. 3). Specifically, due to lowest total leaf areas, the lowest daily amount of C was stored by Ginkgo, followed by Chinese pine (noting the higher leaf photosynthetic rates in these two tree species). With the increase of light intensity, the photosynthetic C sequestration of all tree species increased rapidly from 7:00, reaching maximum values between 9:00 to 9:30, and decreased gently from 10:00 to 16:00 to reach minimum values, thereafter continuing to rise until 17:00 in plant-growing season except for continuing to decrease until 17:00 in

October. As for July and August, the photosynthetic C sequestration of almost all tree species experienced bimodal consecutive decreases between 9:00 and 15:30 (Fig. 3).

Carbon Sinks of Vegetation and Carbon Sources of Traffic in the Contributing Area

Three 40×50 m forest sample plots were selected randomly in the study area, and the average number of trees was counted according to species. Specifically, Amur cork was 160, Chinese ash was 84, Chinese pine was 157, goldenrain was 114, mono maple was 109 and ginkgo was 59. Then, using remote-sensing image

Table 1. Leaf area index (LAI), crown area and total leaf area of single tree of six species.

Species	LAI	Crown area (C)/m ²	Total leaf area of single tree (S)/m ²
Goldenrain	2.303±0.106a	6.252±0.524d	14.398±2.845c
Chinese Ash	2.167±0.134a	4.258±0.236e	9.227±1.632d
Amur Corktree Bark	1.138±0.121c	16.125±1.191a	18.35±2.473b
Mono Maple	1.755±0.095b	12.675±2.355b	22.245±2.834a
Chinese Pine	1.825±0.133b	4.255±0.313e	7.765±1.365e
Ginkgo	0.878±0.126c	8.756±0.721c	7.688±1.126e

Data are means±SE (n = 5). Different letters in the same column indicate significantly different means (p<0.05, Tukey's test)

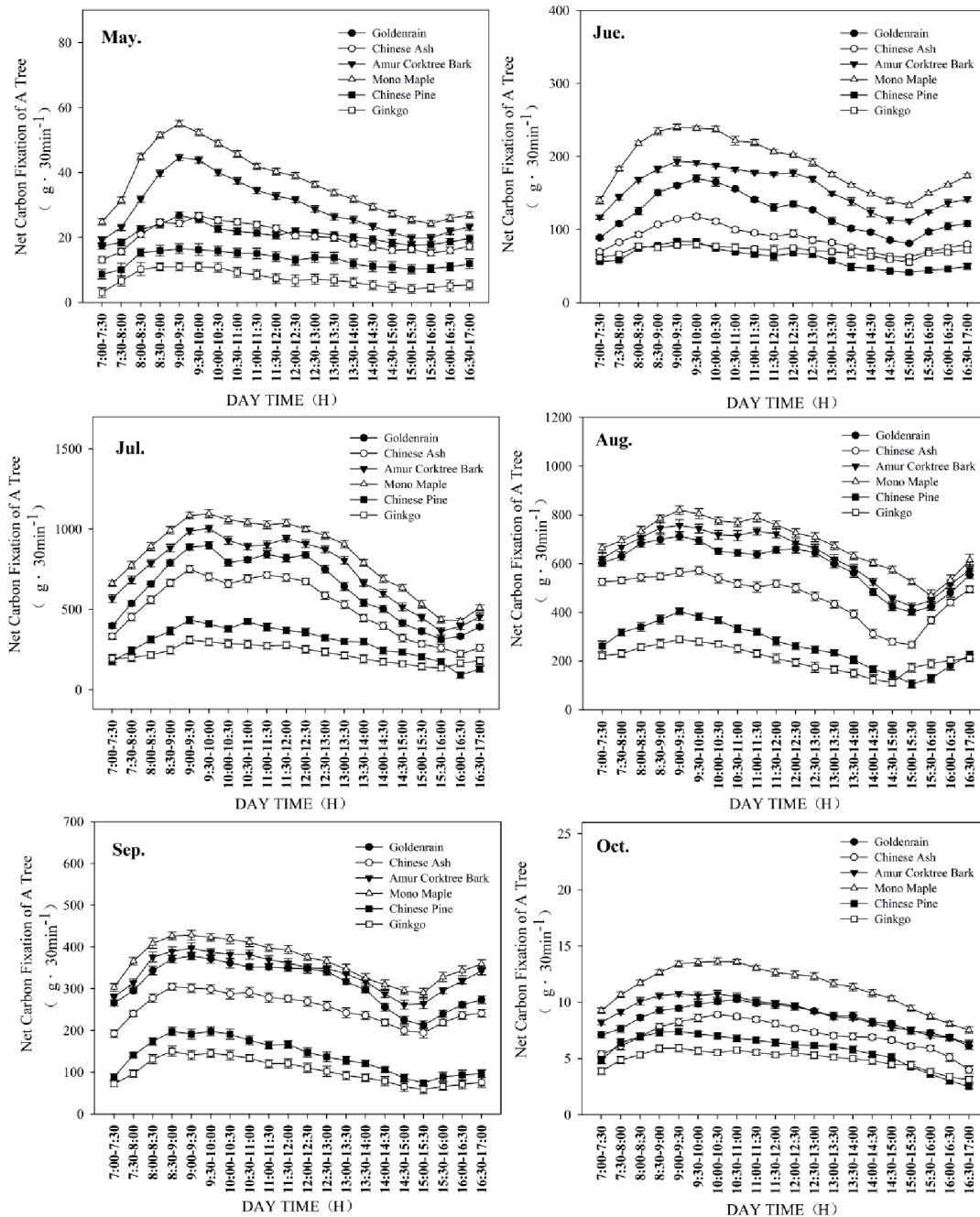


Fig. 3. Characteristics of the daily variation in photosynthetic carbon sequestration per plant in plant-growing season (May-October).

interpretation with 0.5 m accuracy from the Quick Bird satellite on September 4, 2016 and field screening in ArcGIS 10.4 software, we determined the number of trees of all species in the contributing area and calculated the total C sequestration by the vegetation per 30 min (Fig. 4). So, situ monitoring in sample plots was representative and could be expanded to the study area.

As seen from Fig. 4, within the maximum C-flux contribution range during the observation period (7:00-17:00), the trend of the total C sequestration by all trees per 30 min showed a bimodal peak in July and August, but a single peak in other months, which all have different degrees of increase in C

sequestration between 15:00 to 17:00. Obviously, the order of net CO₂ fixation of vegetation was July (123.94-333.92 ton·km⁻²·30 min⁻¹) > August (134.37-268.63 ton·km⁻²·30 min⁻¹) > September (80.53-138.89 ton·km⁻²·30 min⁻¹) > June (34.73-64.01 ton·km⁻²·30 min⁻¹) > May (6.36-12.87 ton·km⁻²·30 min⁻¹) > October (2.16-4.12 ton·km⁻²·30 min⁻¹) during the observation period (7:00-17:00) of plant-growing season (May-

As shown in Fig. 4, there was a significant daytime shift in high-speed traffic flow in the maximum C-flux contribution during the daytime monitoring period (7:00-17:00) of plant-growing season (May-

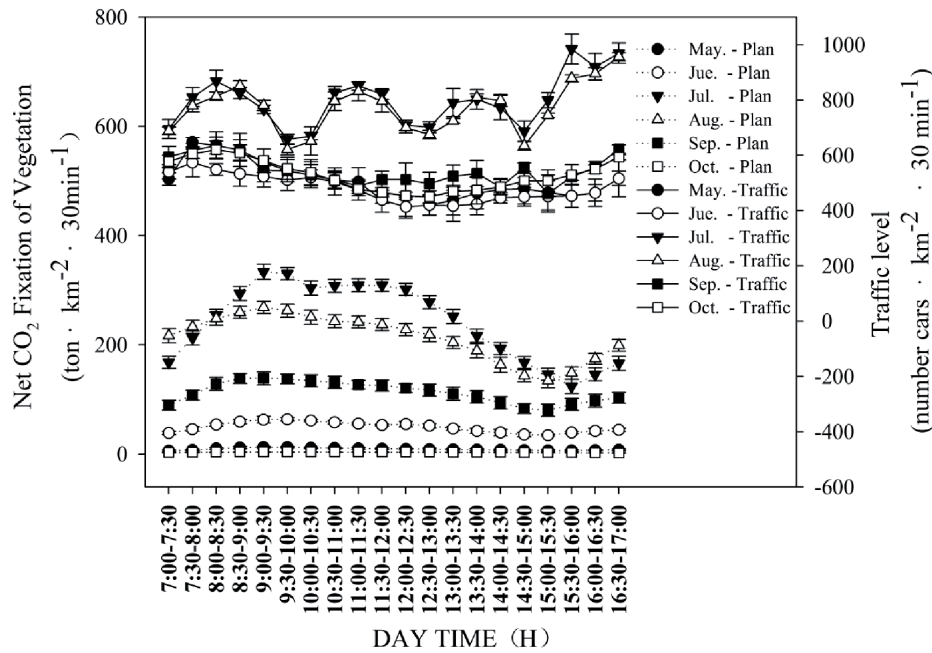


Fig. 4. Characteristics of the daily variation in vegetation carbon sequestration and traffic flow in plant-growing season (May-October).

October). Specifically, traffic flow in July and August showed trends of four peaks (8:00-8:30, 11:00-11:30, 13:30-14:00, 16:30-17:00) and had nearly 30% more traffic flow than other months due to being in tourism-peak season of summer vacation. For other months in non-tourism season, the traffic flow reached its peak quickly between 7:30 to 8:30 and then gradually decreased to the lowest point between 12:00 to 12:30, finally continuing to rise in a fluctuating manner until 17:00.

Correlation between Traffic CO₂ Emissions and Total CO₂ Emissions

Using the C flux formula, we calculated the total amount of C sequestered per 30 min using the C flux per

30 min monitoring data and the maximum contribution area of the underlying vegetation to calculate the total C emissions per 30 min. Then, traffic flow was obtained by visual interpretation of the number of vehicles per 30 min. The questionnaire survey and the IPCC (2007) data were used to determine the CO₂ emission factors for the various models from the vehicle CO₂ emission factors multiplied by the number of each vehicle in the above field-monitored flux contribution area every 30 min to get the total CO₂ emissions from traffic per 30 min within the flux contribution region. Finally, the correlation between the CO₂ emissions from traffic per 30 min and the total C emissions per 30 min calculated using the C flux formula was studied. Fig. 5 shows that there was a significant positive correlation between the traffic flow per 30 min and the total C emissions per 30 min ($R^2 = 0.73$) (Fig. 5). This result indicates that the CO₂ discharged by traffic can nearly represent the total CO₂ emissions, which means that the CO₂ is mainly contributed by traffic emissions.

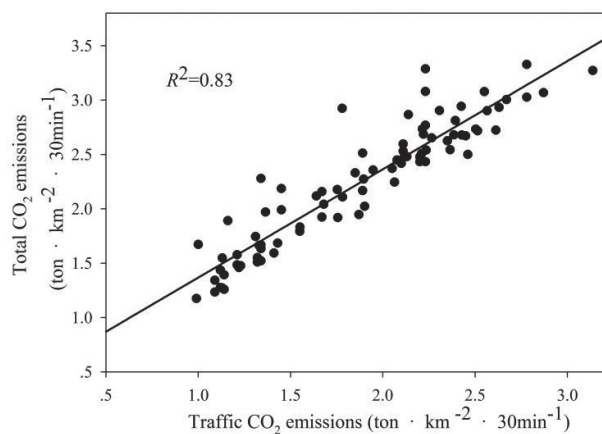


Fig. 5. Correlation between traffic CO₂ emissions and total CO₂ emissions in study area.

Contribution Rate of the Total Carbon Sequestration Factor

Multiple regression analysis was performed to determine which parameters best explained the change in total C sequestration during the daytime monitoring period (7:00-17:00) of plant-growing season (May-October). Based on the results of the analysis, the three main parameters of photosynthetically active radiation, traffic flow and humidity accounted for 92.3% of the change in the total C sequestration by the vegetation (Table 2) during the daytime monitoring period (7:00-17:00) of the plant-growing season (May-October). Except for the constants in the model,

Table 2. Regression analyses pooling all parameters for the plant-growing season (May- October).

	Constant(a)	I (b)	TL(c)	H (d)
Cumulative R ²		0.725	0.892	0.923
Coefficient	2.419	18.091	10.015	-4.415
SC		0.712	0.354	-0.171
P	0.334	0.000	0.000	0.018

Data are mean values. VCF:vegetation carbon fixation (g·30 min⁻¹); I:Irradiance (μmol·m⁻²·s⁻¹); TL:Traffic level (number); H:Humidity (%)

Form of equation: $VCF = a + I*b + TL*c + H*d$

all of the parameters and regression coefficients were significant at the $p < 0.05$ level. Based on the standard coefficient (SC) of these parameters, the total C sequestration by the vegetation was largely influenced by the variables in the order of photosynthetically active radiation > traffic flow > relative humidity, and the total C sequestration was significantly positively correlated with photosynthetically active radiation and vehicle flow and significantly negatively correlated with relative humidity.

Discussion

It is well known that the absorption of CO₂ by vegetation is mainly affected by interacting factors, including leaf area, leaf photosynthetic rate, canopy structure, vegetation type and biomass, plant density, and microclimate [55].

In general, the C sequestration capacity of the tree species using the net photosynthetic C fixation rate per tree follows the order of Mono maple > Amur cork tree > Goldenrain > Chinese ash > Chinese pine > Ginkgo during the daytime monitoring period (7:00-17:00) of the plant-growing season (May-October). This shows that the C sequestration ability of an individual plant is not only based on the amount of C sequestered per unit leaf area, but is also influenced by the leaf area index and the canopy [33,56]. The results of this study indicate that the accumulation of C in tree species mainly occurred in the morning and the species with a relatively high peak accumulation value, such as Mono maple and Amur cork tree, have a stronger photosynthetic ability, that is, greater C assimilation and accumulation per unit leaf area, as well as a greater whole-plant C sequestration capacity and ability.

In addition, it is important to explore the factors driving vegetation C sequestration to sequester more CO₂ and mitigate climate change [31]. In this study, the results of multiple regression analysis showed that the photosynthetic C sequestration effect was mainly related to photosynthetically active radiation, traffic flow and relative humidity (Table 2), which collectively explained 92.3% of the total C sequestration by the vegetation

during the daytime monitoring period of plant-growing season (May-October). However, there was no detectable effect of atmospheric CO₂ concentration and temperature on the total C sequestration of the vegetation, which may be because photosynthetically active radiation and temperature are positively correlated. In other words, the temperature increases with increasing light radiation.

As for atmospheric CO₂ concentration, the traffic flow in July and August were significantly heavier than other months (Fig. 4), but the atmospheric CO₂ concentration did not increase with the increase in traffic flow (Fig. 2d). On the contrary, the atmospheric CO₂ concentration was relatively lower in July and August than other months except June between 11:00-17:00 (Fig. 2d), but the total vegetation photosynthetic C sequestration in July and August was significantly higher than in any other months (Fig. 4). Therefore, it can be concluded that an increase in traffic flow may not raise the concentration of carbon dioxide in the air, but would accelerate the rate of photosynthetic C sequestration by the vegetation under sufficient photosynthetically active radiation because vehicle CO₂ emissions have a fertilization effect [57,58]. What's more, although the light radiation in September was weaker than that in May and June (Fig. 2a), the vegetation C sequestration in September was much more than that in May and June (Fig. 4), which may be due to an increase in CO₂ emitted by traffic flow having a fertilization effect on photosynthesis. A large number of studies have shown that a short-term increase in CO₂ will significantly improve the leaf photosynthetic rate, reducing the photosynthetic induction time and the consumption of CO₂ after illumination, so as to increase the amount of C sequestered by the vegetation [41, 59].

According to the result of regression analyses of vegetation carbon fixation (Table 2), relative humidity was negatively correlated with C sequestration. The reason is that the relatively rapid increase in humidity may lead to a decrease in the transpiration rate, thereby reducing nutrient inputs to the leaves and causing the transpirational flux to decrease and the nutrient supply to the foliage to decline. As a result, the changes in leaf nutritional status brought about a considerable decline in photosynthetic capacity [60].

Conclusions

In this study, the net photosynthetic C fixation was used to measure the C sequestration capacity of different tree species, which mainly occurred in the morning, and the order was Mono maple > Amur cork tree > Goldenrain > Chinese ash > Chinese pine > Ginkgo during the daytime monitoring period (7:00-17:00) of plant-growing season (May-October). Moreover, the main factors controlling photosynthetic C sequestration were photosynthetically active radiation, traffic volume and relative humidity, which accounted for 92.3% of the total C sequestered by the vegetation, and sequestration

was positively correlated with photosynthetically active radiation and traffic flow but negatively correlated with relative humidity. Notably, the CO₂ emitted by traffic will significantly increase the amount of photosynthetic C sequestration, which is called the fertilization effect. It is therefore necessary to promote the planting of trees with a high capacity for C sequestration, such as Mono maple and Amur cork tree, on both sides of roads.

Acknowledgements

This paper was supported by the Research on The Process and Influence Mechanism of Carbon Dioxide Emissions in Different Areas of Beijing Based on Flux Footprint (Grant No. 41771182). The authors gratefully acknowledge Professor Zha Tianshan from Beijing Forestry University, China for providing the CO₂ flux data and thank everyone, including anonymous reviewers, who provided helpful suggestions and critical comments on the manuscript.

Conflict of Interest

The authors declare no conflict of interest.

References

- CETIN M., SEVIK H., Measuring the Impact of Selected Plants on Indoor CO₂ Concentrations. *Polish Journal of Environmental Studies*, **25**, 973, **2016**.
- TURKYILMAZ A., SEVIK H., CETIN M., AHMAIDA SALEH E.A., Changes in Heavy Metal Accumulation Depending on Traffic Density in Some Landscape Plants. *Pol. J. Environ. Stud.*, **27**, 2277, **2018**. DOI: 10.15244/pjoes/78620, <http://www.pjoes.com/Changes-in-Heavy-Metal-Accumulation-Depending-non-Traffic-Density-in-Some-Landscape,78620,0,2.html>
- SEVIK H., OZEL H.B., CETIN M., OZEL H.U., ERDEM T., Determination of changes in heavy metal accumulation depending on plant species, plant organism, and traffic density in some landscape plants. *Air Quality, Atmosphere & Health (Air QualAtmos Health)*, **2018**. <https://doi.org/10.1007/s11869-018-0641-x>
- TURKYILMAZ A., CETIN M., SEVIK H., ISINKARALAR K., AHMAIDA SALEH E.A., Variation of heavy metal accumulation in certain landscaping plants due to traffic density. *Environment, Development and Sustainability*. **2018**. DOI: <https://doi.org/10.1007/s10668-018-0296-7><https://link.springer.com/article/10.1007%2Fs10668-018-0296-7>
- CETIN M., SEVIK H., SAAT A., Indoor Air Quality: the Samples of Safranbolu Bulak Mencilis Cave. *Fresenius Environmental Bulletin*, **26**, 5965, **2017**.
- CETIN M., SEVIK H., ISINKARALAR K., Changes in the particulate matter and CO₂ concentrations based on the time and weather conditions: the case of Kastamonu, *Oxidation Communications*, **40**, 477, **2017**.
- CETIN M., Change in Amount of Chlorophyll in Some Interior Ornamental Plants, *Kastamonu University Journal of Engineering and Sciences*, **3**, 11, **2017**.
- CETIN M., AHMAIDA E.A., MOSSI M.M.M., SEVIK H., The effect of the amount of CO₂ on *Sansevieria trifasciata* in indoor environment. The 3rd International Symposium on Euro Asian Biodiversity, 05-08 July, **2017**, Minsk, Belarus.
- SEVIK H., AHMAIDA E.A., CETIN M., Chapter 31: Change of the Air Quality in the Urban Open and Green Spaces: Kastamonu Sample. *Ecology, Planning and Design*. Eds: Irina Koleva, UlkuDumanYuksel, Lahcen Benaabidate, St. Kliment Ohridski University Press, ISBN: 978-954-07-4270-0, 409, **2017**.
- CETIN M., SEVIK H., "Indoor quality analysis of CO₂ for Kastamonu University", Conference of the International Journal of Arts & Sciences, CD-ROM. ISSN: 1943-6114, **09** (03), 71, **2016**.
- NASA 2014. Global Climate Change: Vital Signs of the Planet. Available at: <http://climate.nasa.gov/400ppmquotes> [accessed December 4, **2014**].
- WEISSERT L.F., SALMOND J.A., SCHWENDENMANN L., A review of the current progress in quantifying the potential of urban forests to mitigate urban CO₂ emissions. *Urban Clim*, **100**, 8, **2014**. doi:10.1016/j.uclim.2014.01.002.
- IPCC 2013. "Summary for Policymakers", in *Climate Change 2013: The Physical Science Basis*. Contribution of Working Group I to the Fifth Assessment Report of the Intergovernmental Panel on Climate Change, eds T.F. Stocker, D.Qin, G.K. Plattner, M. Tignor, S.K. Allen, J. Boschung, et al. New York, NY: Cambridge University Press.
- DOBBS C., ESCOBEDO F.J., ZIPPERER W.C., A framework for developing urban forestecosystem services and goods indicators. *Landsc. Urban Plan*, **99**, 196, **2011**.
- NRC, **2010**. *Advancing the Science of Climate Change*. National Research Council, The National Academies Press, Washington, DC.
- DHAKAL S., Urban energy use and carbon emissions from cities in China and policy implications. *Energ. Policy*, **37**, 4208, **2009**. doi:10.1016/j.enpol.2009.05.020.
- IEA, **2013**. *World Energy Outlook*. International Energy Agency, Paris.
- IPCC, **2007**. *Summary for Policymakers of Climate Change 2007: the Physical Science Basis*. Contribution of Working Group I to the Fourth Assessment Report of the Intergovernmental Panel on Climate Change. Cambridge University Press, Cambridge.
- Beijing Municipal Bureau of Statistics. Available at: <http://www.bjstats.gov.cn/> [accessed December 20, **2017**].
- UNEP, **2014**. *The Emissions Gap Report*.
- DIAZ-PORRAS D.F., GASTON K.J., EVANS K.L., 110 years of change in urban tree stocks and associated carbon storage. *Ecol. Evol.*, **4**, 1413, **2014**. doi:10.1002/ece3.1017.
- MIEHLE P., LIVESLEY S.J., FEIKEMA P.M., LI C., ARNDT S.K., Assessing productivity and carbon sequestration capacity of eucalyptus globulus plantations using the process model Forest-DNDC: calibration and validation. *Ecol. Modell.* **192**, 83, **2006**. doi:10.1016/j.ecolmodel.2005.07.021.
- CAIFIRE, U.S.F.S., **2014**. *Urban Forest Project protocol revision*. <http://www.climateactionreserve.org/how/protocols/urban-forest/rev/> (accessed 14.07.03).
- LIU C., LI X., Carbon storage and sequestration by urban forests in Shenyang, China. *Urban For Urban Green*, **11**, 121, **2012**.
- ZHAO M., KONG Z., ESCOBEDOF.J., GAO J., Impacts of urban forests on offsetting carbon emissions from

- industrial energy use in Hangzhou, China. *J. Environ. Manage.*, **91**, 807, **2010**.
26. GUAN D.S., CHEN Y.J., Roles of urban vegetation on balance of carbon and oxygen in Guangzhou, China. *Journal of Environmental Sciences- China*, **15**, 155, **2003**.
27. NOWAK D.J., CRANE D.E., Carbon storage and sequestration by urban trees in the USA. *Environ. Pollut.*, **116**, 381, **2002**. doi:10.1016/S0269-7491(01)00214-7.
28. MCPHERSON E.G., SIMPSON J.R., PEPPER P.J., AGUARON E. Urban Forestry and Climate Change. USDA Forest Service, Pacific Southwest Research Station, **2008**, Albany, USA.
29. RUSSO A., ESCOBEDO F.J., TIMILSINA N., ZERBE S., Transportation carbon dioxide emission offsets by public urban trees: a case study in Bolzano, Italy. *Urban For. Urban Greening*, **14**, 398, **2015**. doi:10.1016/j.ufug.2015.04.002.
30. TIGGES J., CHURKINA G., LAKES T. Modeling above-ground carbon storage: a remote sensing approach to derive individual tree species information in urban settings. *Urban Ecosyst.*, **20**, 97, **2017**.
31. GRATANI L., VARONE L., Atmospheric carbon dioxide concentration variations in Rome: relationship with traffic level and urban park size. *Urban Ecosyst.* **17**, 501, **2014**. doi:10.1007/s11252-013-0340-1.
32. VELASCO E., ROTH M., NORFORD L., MOLINA L.T., Does urban vegetation enhance carbon sequestration? *Landscape Urban Plann.* **148**, 99, **2016**. doi:10.1016/j.landurbplan.2015.12.003.
33. BISWAS S., BALA S., MAZUMDAR A., Diurnal and seasonal carbon sequestration potential of seven broadleaved species in a mixed deciduous forest in India. *Atmos. Environ.*, **89**, 827, **2014**. doi:10.1016/j.atmosenv.2014.03.015.
34. CHEN W.Y., The role of urban green infrastructure in offsetting carbon emissions in 35 major Chinese cities: a nationwide estimate. *Cities*, **44**, 112, **2015**. Doi:10.1016/j.cities.2015.01.005
35. REYNOLDS C.C., ESCOBEDO F.J., CLERICI N., Does "greening" of neotropical cities considerably mitigate carbon dioxide emissions? The case of Medellin, Colombia. *Sustainability*, **9**, 785, **2017**. doi:10.3390/su9050785
36. BELLUCCO V., MARRAS S., GRIMMOND C.S.B., JARVI L., SIRCA C., SPANO D., Modelling the biogenic CO₂ exchange in urban and non-urban ecosystems through the assessment of light-response curve parameters. *Agricultural and Forest Meteorology*, **236**, 113, **2017**.
37. MURAOKA H., KOIZUMI, H., Photosynthetic and structural characteristics of canopy and shrub trees in a cool-temperate deciduous broadleaved forest: implication to the ecosystem carbon gain. *Agric. Forest Meteorol.*, **134**, 39, **2005**. doi:10.1016/j.agrformet.2005.08.013.
38. BALDWIN N., GILANI O., RAJA S., BATTERMAN S., GANGULY R., HOPKE P., BERROCAL V., ROBINS T., HOOGTERP S., Factors affecting pollutant concentrations in the near-road environment. *Atmos. Environ.*, **115**, 223, **2015**. doi:10.1016/j.atmosenv.2015.05.024.
39. GURNEY K.R., MENDOZA D.L., ZHOU Y.Y., FISCHER M.L., MILLER C.C., GEETHAKUMAR S., DE LA RUE DU CAN S., High Resolution Fossil Fuel Combustion CO₂ Emission fluxes for the United States. *Environ. Sci. Technol.*, **43**, 5535, **2009**. doi:10.1021/es900806c.
40. RILEY M., DUREN C.E.M., Measuring the carbon emissions of megacities. *Nat. Clim. Change*, **2**, 560, **2012**.
41. TOMIMATSU H., TANG Y., Effects of high CO₂ levels on dynamic photosynthesis: carbon gain, mechanisms, and environmental interactions. *J. Plant Res.*, **129**, 365, **2016**. doi:10.1007/s10265-016-0817-0.
42. GIOLI B., GUALTIERI G., BUSTILLO C., CALASTRINI F., ZALDEI A., TOSCANO P., Improving high resolution emission inventories with local proxies and urban eddy covariance flux measurements. *Atmospheric Environment*, **115**, 246, **2015**.
43. CHRISTEN A. Atmospheric measurement techniques to quantify greenhouse gas emissions from cities. *Urban Clim.*, **10**, 241, **2014**. doi:10.1016/j.uclim.2014.04.006.
44. VACCARI F.P., GIOLI B., TOSCANO P., PERRONE C., Carbon dioxide balance assessment of the city of Florence (Italy), and implications for urban planning. *Landscape and Urban Planning*, **120**, 138, **2013**.
45. LI Y., WANG Z., WANG F., DONG S.C., LI Z.H., A review of assessment methods, influencing factors and process on urban carbon emissions. *J. Nat. Res.*, **28**, 1637, **2013**.
46. VELASCO E., ROTH M., TAN S.H., QUAK M., NABARRO S.D.A., NORFORD L., The role of vegetation in the CO₂ flux from a tropical urban neighbourhood. *Atmos. Chem. Phys.* **13**, 10185, **2013**. doi:10.5194/acp-13-10185-2013.
47. ZHA T.S., KELLOMAKIS., WANG K.Y., ROUVINEN I., Carbon sequestration and ecosystem respiration for 4 years in a Scots pine forest. *Glob. Change Biol.*, **10**, 1492, **2004**. doi:10.1111/j.1365-2486.2004.00835.x.
48. CHEN B.Z., BLACK T.A., COOPS N.C., HILKER T., TROFYMOW J.A., MORGENSTERN K., Assessing tower flux footprint climatology and scaling between remotely sensed and eddy covariance measurements. *Boundarylayer Meteorol.* **130**, 137, **2009**. doi:10.1007/s10546-008-9339-1.
49. VAN ULDEN A.P., Simple estimates for vertical diffusion from sources near the ground. *Atmos. Environ.*, **12**, 2125, **1978**. doi:10.1016/0004-6981(78)90167-1.
50. GRYNING S.E., HOLTSLAG A.A.M., IRWIN J.S., SIVERTSEN B. Applied dispersion modelling based on meteorological scaling parameters. *Atmos. Environ.*, **21**, 79, **1987**. doi:10.1016/0004-6981(87)90273-3.
51. FINN D., LAMB B., LECLERC M.Y., HORST T.W., Experimental evaluation of analytical and Lagrangian surface-layer flux footprint models. *Boundarylayer Meteorol.* **80**, 283, **1996**.
52. KORMANN R., MEIXNER F.X., An analytic footprint model for neutral stratification. *Boundarylayer Meteorol.* **99**, 207, **2001**. doi:10.1023/A:1018991015119.
53. LI Y., ZHENG J., LI Z.H., YUAN L., YANG Y., LI F.J., Re-estimating CO₂ emission factors for gasoline passenger cars adding driving behaviour characteristics. A case study of Beijing. *Energ. Policy*, **1021**, 353, **2017**.
54. WANG Z.J., Research on vegetation quantity and carbon-fixing and oxygen-releasing effects of Fuzhou Botanical Garden. *Chinese Landscape Architecture*, **26**, 1, **2010**.
55. BALDOCCHI D.D., WILSON K.B., GU L. How the environment, canopy structure and canopy physiological functioning influence carbon, water and energy fluxes of a temperate broad-leaved deciduous forest--an assessment with the biophysical model CANOAK. *Tree Physiol.*, **22**, 1065, **2002**. doi:10.1093/treephys/22.15-16.1065.
56. BREDA N.J. Ground-based measurements of leaf area index: a review of methods, instruments and current controversies. *J. Exp. Bot.*, **54**, 2403, **2003**. doi:10.1093/jxb/erg263.
57. REDDY A.R., RASINENI G.K., RAGHAVENDRA A.S. The impact of global elevated CO₂ concentration on

- photosynthesis and plant productivity. *Curr. Sci.*, **99**, 46, **2010**.
58. LEUZINGER S., HATTENSCHWILER S. Beyond global change: lessons from 25 years of CO₂ research. *Oecologia*, **171**, 639, **2013**. doi: 10.1007/s00442-012-2584-5.
59. XU Z.Z., JIANG Y.L., ZHOU G.S. Response and adaptation of photosynthesis, respiration, and antioxidant systems to elevated CO₂ with environmental stress in plants. *Frontiers in Plant Science*, **6**, 1, **2015**. doi:10.3389/fpls.2015.00701.
60. SELLIN A., TULLUS A., NIGLAS A., OUNAPUU E., KARUSION A., LOHMUS K. Humidity-driven changes in growth rate, photosynthetic capacity, hydraulic properties and other functional traits in silver birch (*Betula pendula*). *Ecol. Res.*, **28**, 523, **2013**. doi:10.1007/s11284-013-1041-1.